Bull Volcanol (1993) 55:523–535

Bulletin of Volcanology

A case of no-wind plinian fallout at Pululagua caldera (Ecuador): implications for models of clast dispersal

Paolo Papale[1], **Mauro Rosi**[2]

[1] GNV, Universita' di Pisa, Via Santa Maria 53, I-56126 Pisa, and Istituto Nazionale di Geofisica, Roma, I-Italy.
[2] Dipartimento di Scienze della Terra, Via Santa Maria 53, I-56126 Pisa, Italy

Received May 1, 1991/Accepted April 2, 1993

Abstract. The caldera of Pululagua is an eruptive centre of the Northern Volcanic Zone of the South American volcanic arc, located about 15 km north of Quito, Ecuador. Activity leading to formation of the caldera occurred about 2450 b.p. as a series of volcanic episodes during which an estimated 5–6 km^3 (DRE) of hornblende-bearing dacitic magma was erupted. A basal pumice-fall deposit covers more than 2.2×10^4 km^2 with a volume of about 1.1 km^3 and represents the principal and best-preserved plinian layer. Circular patterns of isopachs and pumice, lithic and Md isopleths of the Basal Fallout (BF) around the caldera indicate emplacement in wind-free conditions. Absence of wind is confirmed by an ubiquitous, normally graded, thin ash bed at the top of the lapilli layer which originated from slow settling of fines after cessation of the plinian column (co-plinian ash). The unusual atmospheric conditions during deposition make the BF deposit particularly suitable for the application and evaluation of pyroclast dispersal models. Application of the Carey and Sparks' (1986) model shows that whereas the 3.2-, 1.6-, and 0.8-cm lithic isopleths predict a model column height of about 36 km, the 6.4-cm isopleth yields an estimate of only 21 km. The 4.9- and 6.4-cm isopleths yield a column height of 28 km using the model of Wilson and Walker (1987). The two models give the same mass discharge rate of 2×10^8 kg s^{-1}. A simple exponential decrease of thickness with distance, as proposed by Pyle (1989) for plinian falls, fits well with the BF. Exponential decrease of size with distance is followed by clasts less than about 3 cm, suggesting, in agreement with Wilson and Walker (1987), that only a small proportion of large clasts reach the top of the column. Variations with distance in clast distribution patterns imply that, in order to obtain column heights by clast dispersal models, the distribution should be known from both proximal and distal zones. Knowledge of only a few isopleths, irrespective of their distance from the vent, is not sufficient as seemed justified by the method of Pyle (1989).

Correspondence to: M. Rosi

Key words: Ecuadorian volcanism – explosive eruptions – plinian fallout – plinian column – clast dispersal

Introduction

Plinian eruptions are among the most powerful manifestations of volcanic activity. Such events deposit tephra across areas as large as 10^5 km^2, from eruption columns of 10–55 km height, and with discharge rates of up to 10^9 kg s^{-1} (Wilson 1976; Wilson et al. 1978; Settle 1978; Walker 1981). Unlike most explosive styles, in which products are expelled by very unstable processes, plinian eruptions are dominated by substeady discharge of gas and fragmented magma, which allows a quantitative approach to the problems of the formation and evolution of the resulting eruptive column (Wilson 1980). Starting from a theory of the ascent of thermal plumes (Morton et al. 1956), several authors (e.g. Sparks 1986; Carey and Sparks 1986; Wilson and Walker 1987) have developed numerical models that attempt to predict the behaviour of volcanic eruption columns and the characteristics of tephra fall deposits.

Owing to the infrequency of plinian events, only a few eruptions have been accurately observed and documented (Walker 1981). Therefore, most of what we know about them derives from analysis of resultant deposits, i.e. by deductive reasoning. Unfortunately this process is very difficult, because the amount of significant information that can be obtained is smaller than the number of independent variables that describe the process. This implies that many assumptions are necessary, inevitably increasing the uncertainty of the results. For example, at present we are able to model column heights with an approximation of about 10–20% (Woods 1988; Carey and Sigurdsson 1989).

This work is focused on the initial eruption of Pululagua, Ecuador, which led to deposition of a plinian fall layer and associated products about 2500 years b.p.

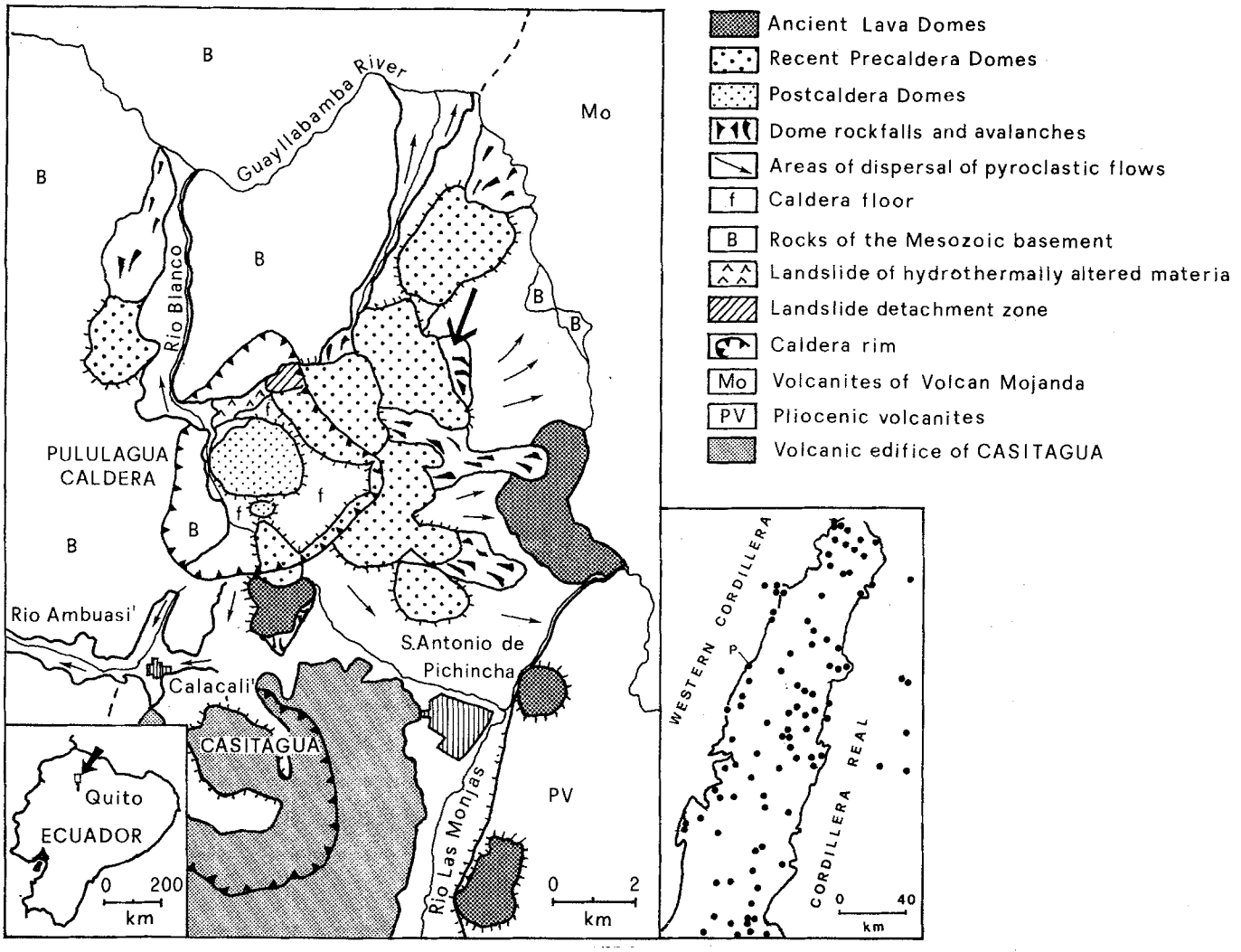

Fig. 1. Geological sketch map of the area of Pululagua caldera. The *thick arrow* indicates the location of the stratigraphic section of Fig. 2. The *figure on the right* shows the location of Quaternary volcanoes (*full circles*), where '*P*' indicates the Pululagua caldera

The basal pumice fall shows characteristics that make it particularly suitable for the application and evaluation of clast dispersal models from plinian columns. Isopachs and isopleths show a nearly circular geometry centred on the vent area, which implies nearly wind-free conditions during the eruption. There are very few documented examples of deposits from such events, making the Pululagua case valuable because the absence of wind removes a variable, the effects of which are difficult to assess.

Geology of the Pululagua caldera

Quilotoa, Guagua Pichincha, Pululagua, Cuicocha and Cerro Negro volcanoes form, from south to north, the active Andean Volcanic Front of Ecuador (Simkin et al. 1981; Barberi et al. 1988). The inception of predominantly explosive activity at these volcanic centres seems to be coeval and points to a very recent renewal of activity at the volcanic front characterized by the rise of volatile-rich magmas (Barberi et al. 1988).

Pululagua, located 15 km north of Quito (Fig. 1), is an irregularly shaped caldera with an area of about 19 km^2 and a subrectangular base at an altitude of about 2500 m. The caldera is surrounded by a group of older lava domes (Recent Precaldera Domes, RPD), and the syncaldera products overlie a sequence of dome rockfalls, rock avalanches, and block-and-ash flows formed in association with extrusion of these lava domes. Most of the RPD lie within a 9 by 4.5 km area elongated in a N-S direction. The vents were probably controlled by normal faults that bound the Interandean Depression to the west, a major graben-like structure that runs parallel to the volcanic front of Ecuador. The caldera is breached on the west along the Rio Blanco valley, but the lack of a pre-existing volcanic edifice suggests that the notch is probably inherited from the pre-volcanic topography rather than the result of a volcanic avalanche.

Due to the irregular topography around the caldera, the difference in height between the rim and the floor is hard to estimate; however, where the morphology seems least uneven, the topographic wall is about

300 m. Two composite postcaldera domes of height 480 m and 200 m occupy the central part of the depression (Fig. 1). They have an estimated combined volume of about 0.6 km^3. The volume of the caldera was estimated at 5.3 km^3, assuming an infilling of about 100 m by subsequent pyroclastic products, particularly those associated with the extrusion of the postcaldera domes. Using an estimated lithic content of 10–30 wt% for all tephra products, as deduced from visual observations, and assuming equal magma and lithic density of 2500 kg m^{-3}, the volume of the magma erupted during caldera-forming explosions is in the range 3.7–4.8 km^3.

Both RPD and the syn- and postcaldera products are mainly dacitic in composition, with a low K_2O content very similar to those typical of tholeiitic trends; however, they are calcalkaline and lack any iron enrichment.

Stratigraphy of caldera-forming and post-caldera volcanics

Erosion by the Rio Blanco has exposed about 100 m of pyroclastic and volcaniclastic deposits, mainly related to extrusion of the postcaldera domes. These products are partially sintered block-and-ash flow deposits made up of non-vesiculated lava clasts which show oxidation indicative of a high-temperature emplacement (Williams 1960; Crandell and Mullineaux 1973). Their total volume is similar to that of the domes, increasing the volume of lava emitted during the postcaldera stage to at least 1 km^3. These block-and-ash flow deposits overlie the complex sequence of the pyroclastic products of the caldera-forming phase.

The inception of the caldera-forming activity is well constrained by recent radiometric data and archaeological studies. Pyroclastic deposits of this phase directly overlie artifacts of the Cotocollao archaeological site located in the northern area of Quito. Excavations indicate that the site was in use for more than 1000 years until 2450 b.p., and was thereafter suddenly abandoned (Villalba 1988). Further chronological information comes from ^{14}C dating performed on plant remains associated with the Pululagua pyroclastics. Radiocarbon dating of peat underlying the basal fall yielded an age of about 2650 b.p. (Geotermica Italiana-INEMIN 1989). Two younger ages of 2285 and 2305 b.p. were obtained on small branches embedded in pyroclastic flow and surge deposits of uncertain stratigraphic position within the Pululagua caldera-forming succession (Hall 1977; Isaacson 1987).

A complex sequence of volcanic eruptions led to caldera collapse. At least ten eruptive episodes have been identified by the presence of minor weathered layers and/or erosive unconformities. Using the relative importance of these horizons (i.e. their thickness and intensity), the pyroclastic beds have been grouped into Lower, Middle and Upper Units (Fig. 2). The basal deposits, the focus of this work, make up the first of

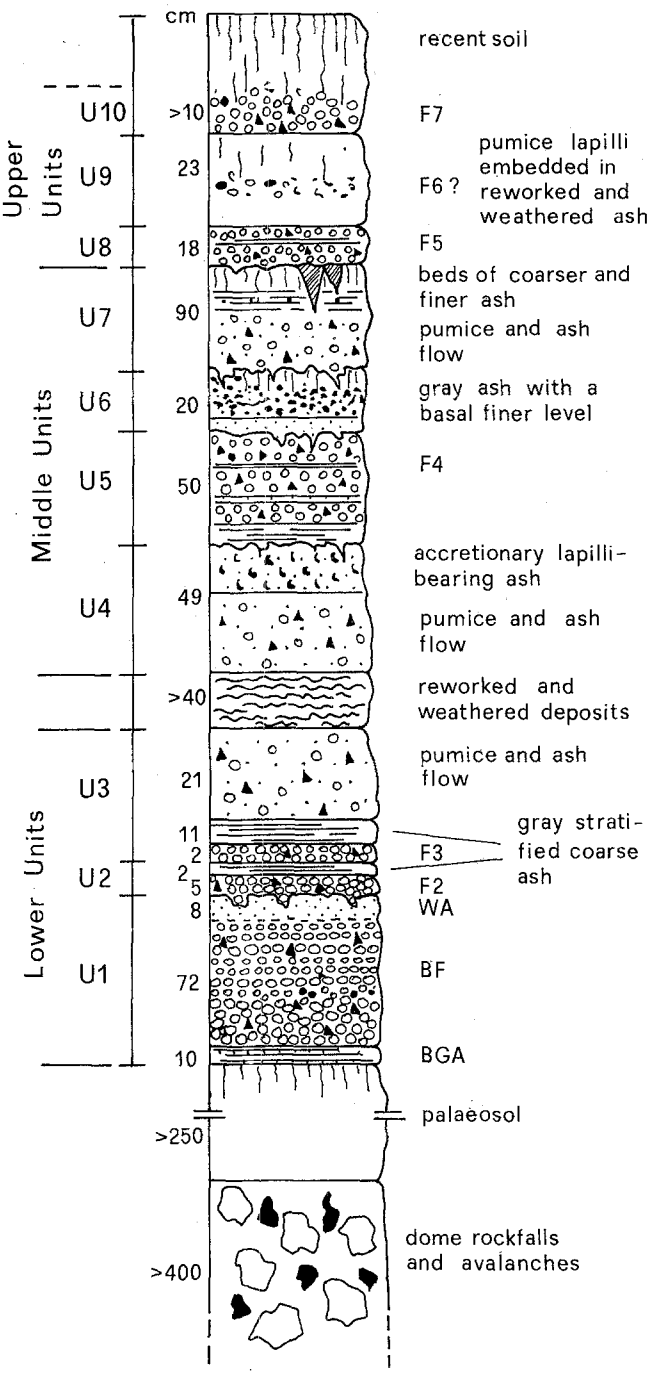

Fig. 2. Stratigraphy and nomenclature of the products of Pululagua caldera-forming eruptions. Location of the section is given in Fig. 1. Eruptive units U1 to U10 are separated from each other by erosive unconformities. BF and F2 to F7 represent plinian and/or subplinian pumice fallout layers. *Numbers* on the left-hand side of the column indicate the thickness in cm. The section is located on a topographic high and lacks most of the valley-ponded pyroclastic flows of the eruptive sequence

the three Lower Units (U1 in Fig. 2). Low-grade ignimbrite and surge deposits are concentrated along valleys around the caldera and in the volcaniclastic apron that extends east and southeast of the caldera towards S. Antonio de Pichincha, attaining a maximum thickness of more than 30 m in the Rio Las Monjas valley

(Fig. 1). Fallout deposits consist of seven plinian pumice layers with intercalated ash beds, each with a thickness less than 1 m. Accumulation is thickest west of the caldera, where the entire tephra blanket exceeds 1 m in thickness at about 35 km from source. According to Isaacson (1987), the impact of the repeated downwind fallouts from Pululagua on human communities was severe as far as the slopes of the Western Cordillera and perhaps as much as 150–200 km toward the coast of Ecuador.

Stratigraphic correlations within the pyroclastic deposits were established using the seven pumice falls as marker beds; the fall units are labelled from bottom to top with numbers from 1 (= Basal Fallout, BF) to 7. Fallout layers 1–5 can be traced fairly easily in the field to 20 km from the caldera rim. Isopachs of layers 2–5 show dispersal patterns towards the west, with slightly different dispersal directions (Fig. 3).

Deposits of the initial eruption

Stratigraphy and lithology

The first syncaldera eruptive unit (U1 in Fig. 2) consists of three tephra layers: a thin, stratified, basal grey ash fall, a plinian pumice fall, and a fine-grained, white ash. The three layers are conformable and are believed to have been erupted and deposited without any significant interruption.

The basal grey ash (BGA) is a fall unit up to 10-cm thick with plane-parallel stratification defined by alternations of coarse and fine ash. The stratification is most evident within 4–5 km of the caldera rim (Fig. 4). This layer is always present below the basal plinian fall SE and NW of vent to more than 20 km from source, but it occurs no further than 10–11 km from vent in the NE direction and 6–7 km towards the S. It consists mostly of juvenile, non-vesiculated fragments (about 50 wt%) and significant amounts (25–30 wt%) of free crystals (amphibole and plagioclase in nearly equal proportion) and pumice (15–20 wt%). Less than 5 wt% of the ejecta are lithic clasts consisting of oxidized lavas and metasedimentary rocks. In some localities the finer beds show thickness variations that are likely to have originated by slight slumping during deposition, as well as a vesicular structure, probably due to the coalescence of damp accretionary lapilli (Rosi 1992), suggesting that the ash was nearly saturated with water at the time of deposition. The high fragmentation (>81 wt% finer than 1 mm in all analysed samples) and the vesiculated texture of the ash suggest that the onset of activity was characterized by several discrete phreatomagmatic explosions (cf Self and Sparks 1978).

The basal plinian fall (BF) is a relatively thin (<1 m), widely dispersed, fall unit. The isopachs are shown in Fig. 5. They show a nearly-circular geometry centered on the vent area, which is interpreted to be due to an almost complete absence of wind during the eruption. The lack of data in the NW sector is due to the presence of thickly forested mountains with no ac-

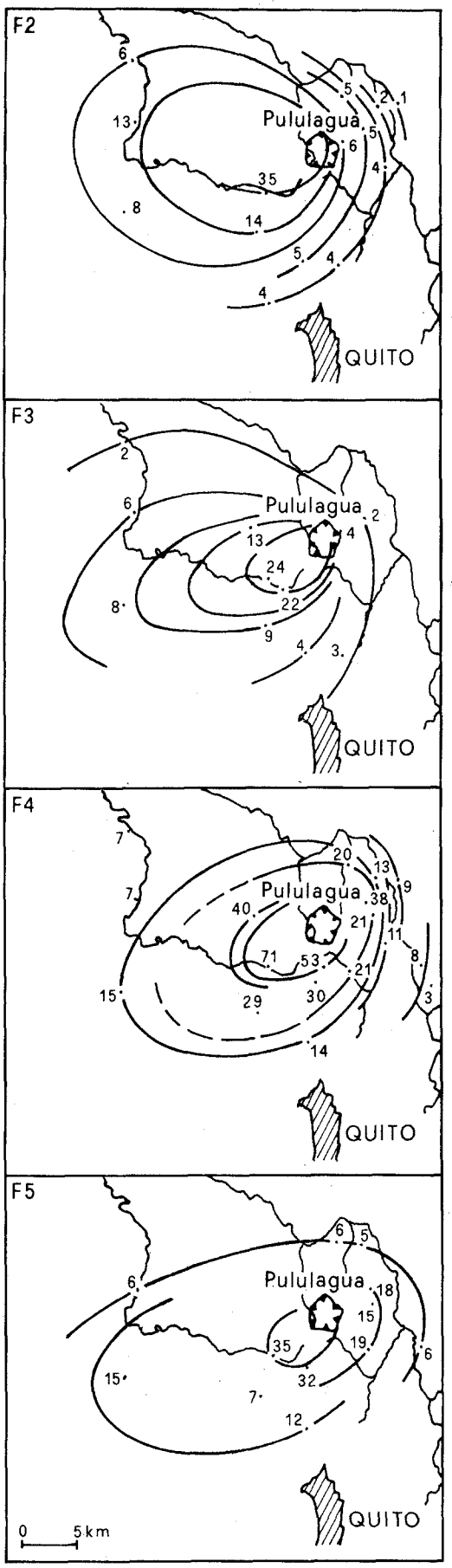

Fig. 3. Isopach maps of the fall layers from 2 to 5. Values are in cm

Fig. 4. Basal eruption sequence of Pululagua 3 km NE of the caldera rim. *BGA,* Basal Gray Ash; *BF,* Basal Fall; *WA,* White Ash; *ITD,* Ignimbrite Type Deposit (see text). *Arrows* indicate finer intervals within the BF. On top of the basal sequence is the thinly stratified F2. *Bar* is 20 cm

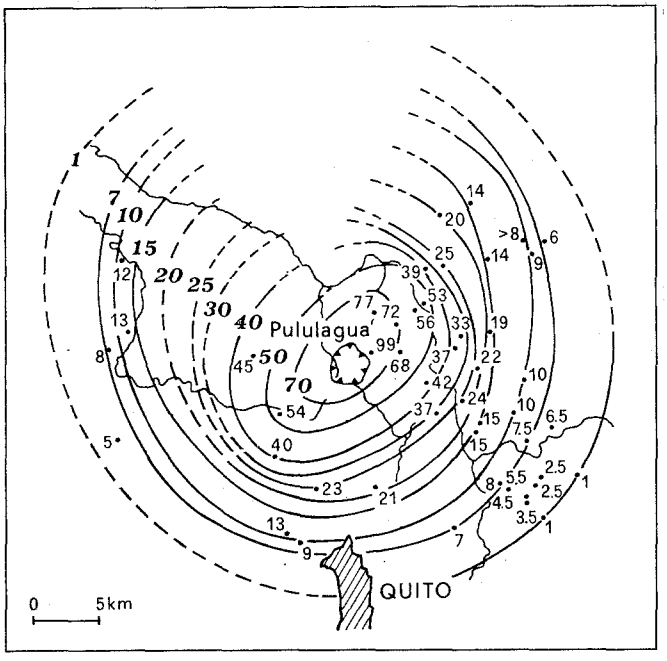

Fig. 5. Isopach map of the Basal Fall (BF) of Pululagua. Values are in cm

cess. BF is usually not graded, except at its top where it grades from lapilli to the overlying white ash. Northeast of the caldera it contains two plane-parallel finer layers each with gradational boundaries, less than 10 cm thick, and made up of the same components (Fig. 4). These finer layers increase in thickness toward the caldera, where they are replaced by surge deposits.

BF contains highly porphyritic pumice clasts with nearly equal quantities of plagioclase (18.8 wt%) and amphibole (23.7 wt%) and subordinate amounts of magnetite (1.54 wt%). The glass is whitish, unlike that of pumice of the overlying fall layers (especially from F4 to F7) which tends to be yellowish to pale brown. The pumice vesicularity ranges from 72 to 80% for clasts in the 32-4 mm range, and is always close to 72% in the 4-1 mm range. This narrow interval of vesicularity suggests that no significant interaction with groundwater took place during the plinian phase (Houghton and Wilson 1989). Lithics represent about 33 wt% of the deposit within the 1-cm isopach, becoming less abundant with decreasing grainsize, which is also in agreement with a purely magmatic plinian eruption (Barberi et al. 1989). Lithics are mostly lavas, both fresh and oxidized, with a subordinate amount of weathered basement sandstone and siltstone. The latter are characteristic of the BF, being virtually absent in the overlying fall layers.

The white ash (WA) is a normally graded, fine-ash layer up to about 10 cm thick that ubiquitously seals the pumice lapilli fallout layer. At 6 km east of the vent, about 97 wt% of the ash is finer than 1 mm, and more than 75 wt% is finer than 1/16 mm. It is made up almost entirely (>80 wt%) of glass shards, with a lower proportion (<20 wt%) of crystals (amphibole and plagioclase in equal proportion), and <1 wt% lithic particles. The transition between the BF and WA is gradual (Fig. 6) and is characterized by a continuos granulometric gradient. This necessarily involves some arbitrary choice about the limit between BF and WA. The boundary between them was placed at a level where only clasts less than 0.5 mm in size were visible in the deposit. We believe that WA originated by the late settling of the progressively finer portion of the material originally contained in the plinian column (co-plinian ash). This origin is supported by its grainsize distribution and, in particular, by the relatively good sorting ($\sigma\phi \leq 2$), which is consistent with a fallout origin. Since primary ignimbrites are lacking and pyroclastic surges are very small, we believe that co-ignimbrite ash did not contribute significantly to the WA. Its distribution is rather uniform over a circular area that exceeds the dispersal of the BF itself, with a thickness of 3–10 cm within a radius of about 30 km.

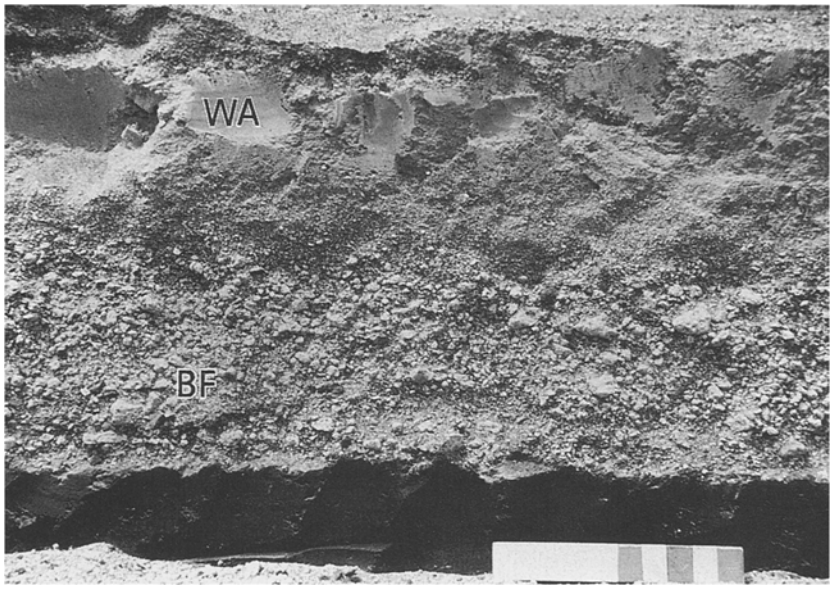

Fig. 6. The Basal Fall layer (*BF*) grades up continuosly into the White Ash (*WA*). *Bar* is 20 cm

Deposits at the foot of steep slopes sometimes include a poorly sorted ($\sigma\phi \geq 3$), decimetre- to metre-thick, ignimbrite-like layer above the WA (ITD in Fig. 4) made up of the same components as the underlying BF, but with a large proportion of white ash matrix (about 20 wt% of the deposit being finer than 0.063 mm). Where it is present, the underlying WA is reduced to a thickness of about 2–3 cm. Since the deposit does not show any evidence of a water-supported resedimentation origin, we conclude that it originated from secondary pyroclastic mass flows resulting from localized slumping of the dry WA and BF. The occurrence of such secondary pyroclastic flows was proposed for the lateral blast surge at Mount St. Helens (Fisher et al. 1987). In the case of Pululagua, the phenomenon seems to have been slightly different in that it involved cold, freshly accumulated, fallout ash on slopes being remobilized by a mechanism akin to snow avalanching. The quiescence that followed the initial eruption is marked by erosional unconformities that usually affect the WA. After a short pause the volcano resumed activity with the eruption of fallout F2.

Volume

Knowledge of the total volume of a tephra deposit is fundamental for defining the magnitude of an eruption. For plinian falls a major obstacle is the difficulty of obtaining distal thickness information. To overcome this problem, various methods have been proposed in the literature (e.g. Rose et al. 1973; Suzuki et al. 1973; Vucetich and Pullar 1973; Howorth 1975; Carey and Sigurdsson 1980; Walker 1980). Different methods are based on various assumptions and mathematical models, and when applied to the same deposit they often yield quite different results (Froggatt 1982). More recently, Pyle (1989) presented a method for computing the volume of a fall deposit assuming an exponential thinning law. This model fits the data from the BF of Pululagua, hence it was preferred to other methods.

Although the data agree very well with a constant exponential thinning law (Fig. 7), the distal portion of the deposit shows a sharp change in slope on the 'ln thickness-area$^{1/2}$' plot which is not found in any of the examples reported by Pyle (1989). This is possibly a consequence of our arbitrary separation between BF and WA, and ideally the model should be applied to the whole fall deposit (i.e. BF + WA). However, our attempt to reconstruct the isopachs of the whole deposit did not give good results, probably because of the difficulty of taking account of erosion and aeolian reworking of the WA. Future studies should examine the distribution pattern of the most distal portions of WA. It is worth noting that, due to the few measurements on the very distal BF, the 1-cm isopach is reconstructed mainly by analogy with the general trend, and it is possible that its real pattern would indicate a greater dispersal.

The point corresponding to 99-cm thickness in Fig. 7 is not a true data point but is an extrapolation

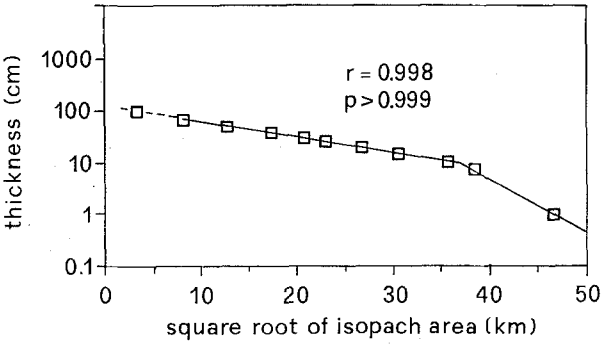

Fig. 7. 'ln Thickness vs square root of isopach area' diagram for the BF (after Pyle 1989). *r*, correlation coefficient; *p*, coefficient of probability of correlation; both refer to the straight line with lower slope. Explanation in the text

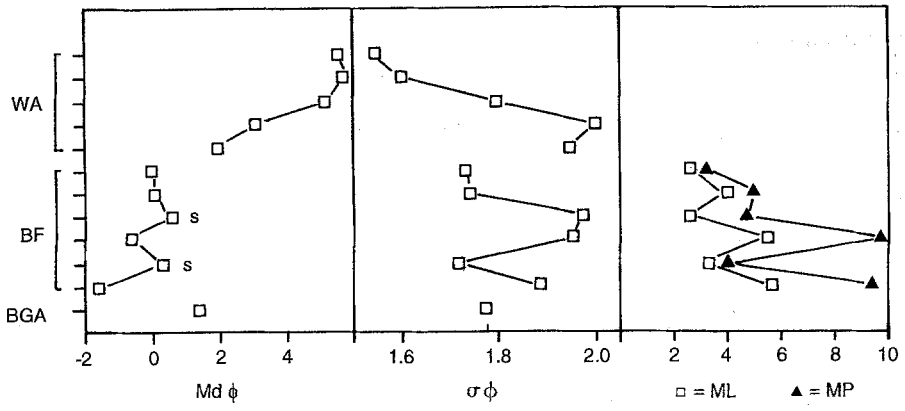

Fig. 8. Representative vertical grainsize variations of the basal sequence. *BGA,* Basal Gray Ash; *BF,* Basal Fallout; *WA,* White Ash; *s,* surge levels. Samples of BGA and BF come from a section located on the northeastern rim of the caldera (about 2 km from the probable position of the vent), with total (BGA + BF) thickness of 90 cm. Samples of WA (total thickness 6 cm) come from a section located about 6 km east of the caldera rim. MP and ML values are in cm

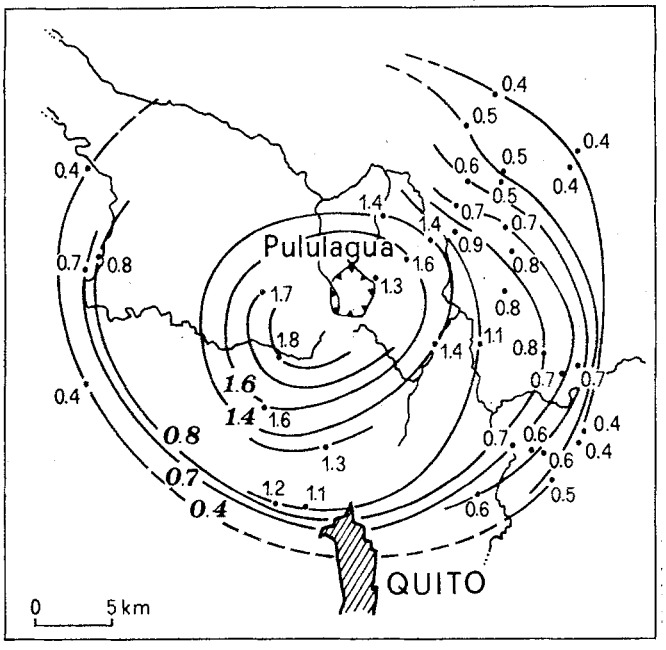

Fig. 9. Isopleth map of the median diameter of grainsize of the BF. Values are in mm

for the only northern proximal section to a circular isopach in accordance with the general trend.

The volume of the BF, as obtained from the 'ln thickness-area$^{1/2}$' plot in Fig. 7, is 0.75 km^3 (DRE = 0.20 km^3). Assuming that the whole deposit (BF + WA) continues to follow a constant exponential thinning trend until it is vanishingly thin, then the total calculated volume rises to about 1.1 km^3 (DRE = 0.34 km^3), with the 1-mm isopach being at a mean distance of about 70 km from the vent.

Grainsize characteristics

Grainsize analyses were carried out on more than 40 samples of BF. Sampling for grainsize distribution was carried out on the entire thickness of BF, but did not include WA.

As already pointed out, in medial to distal outcrops NE of the vent the BF has at least two finer subunits in its middle portion (Fig. 4). In more proximal locations less than 3–4 km from the caldera rim, these subunits become more prominent and are replaced by surge deposits (Fig. 8). The surge horizons are marked by an increase in the Mdϕ value, a decrease in the maximum diameter of pumice (MP) and lithics (ML), and by a wide range of sorting. These are all characteristics that reflect their different emplacement modes with respect to the fall layer. They are possibly due to partial collapses that involved material from the sides of the ascending column (cf Carey et al. 1988).

The WA appears to be a rather uniform layer up to localities 6–7 km away from the caldera. Due to its fine mode, the ash was analysed down to 4-2 microns using a 'Coulter Counter' TA II instrument. The overall normal grading of the BF continues in the WA (Fig. 8). A systematic size study of the WA is a necessary future step for gaining knowledge of the total grainsize distribution as well as for better understanding of the transport and deposition processes of the plinian ash.

The presence of finer layers interfingering with the normal lapilli fall northeast of the vent strongly affects the trend of isopleths for the median diameter of clasts. These show an asymmetrical pattern (Fig. 9) that agrees well with a process of contamination by fines. This effect becomes less evident away from the vent, until it vanishes at about 15 km, as shown by the regular circular pattern of the 0.4-mm isopleth, suggesting that at this distance the influence of the finer material was negligible.

The grainsize characteristics of the BF are similar to those reported in the literature for the plinian deposits (Figs. 10 and 11), with the exception of the trend for median diameter, which is partly due to the above-mentioned contamination by fines. Points in Fig. 10a derived from proximal isopleths tend to be shifted from the plinian field by this contamination, whereas the 0.4-, 0.5- and 0.6-mm isopleths, corresponding to greater distances from the vent, where contamination by fines is absent or weak, lie within the plinian field. If the isopleths of the median diameter are remodelled as circles with a radius equal to their radius in a southwesterly direction (full squares in Fig. 10a), then the discrepancy is greatly reduced. In contrast to the median grainsize, the MP and ML values are unaffected by

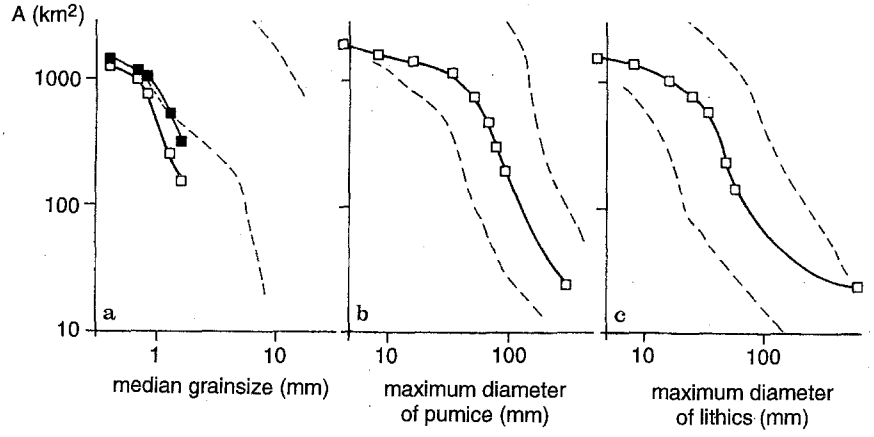

Fig. 10. Diagram 'lnA (area enclosed by each isopleth) vs **a** lnMedian diameter; **b** lnMP; **c** lnML' (all in mm). The *dashed lines* indicate the field of plinian fall deposits (after Walker 1981). *Open squares* refer to the BF layer. *Dark squares* in Fig. 10a refer to the area of isopleths as computed by considering circular patterns with radius equal to that in the SW direction

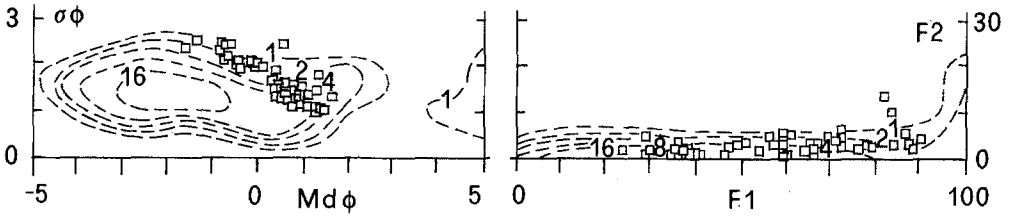

Fig. 11. Comparison between grainsize characteristics of the BF (*open squares*) and the filed of plinian fall layers. *F1*, wt% less than 1 mm, and *F2*, wt% less than 63 μm. Contours after Walker (1983)

contamination by fines and depend only on the maximum height of the column; as a result, the relevant points lie entirely within the plinian field (Fig. 10b, c).

On the 'Mdφ-σφ' diagram (Fig. 11) BF samples lie in the finer grained portion of the fall field; this is partly due to a scarcity of proximal data points, but it probably also reflects an abundance of fines in the collected samples. The value of σφ decreases regularly with increasing Mdφ, displaying rather high values for proximal sites; this feature is once again attributed to the absence of wind. The positive correlation between wind velocity and sorting of fall deposits was already pointed out by Walker (1971). Moreover, the finer top which was included in the sampling of the BF (up to a clast size of 0.5 mm) reduces the median diameter and increases the value of σφ, particularly in proximal sections where the BF is coarse.

Dispersal of pumice and lithic clasts

Maximum grainsize data for the BF were obtained at almost 50 sections around the caldera, down to a thickness of 1 cm. Exceptional preservation is favoured by the dry climate of the Interandean Depression and by the sealing effect of the overlying WA. Maximum diameters of pumice (MP) and lithics (ML) at each location were obtained by averaging the maximum length of the five largest clasts collected on a 0.5 m^2 surface. This procedure follows that described elsewhere (e.g. Carey and Sparks 1986; Carey and Sigurdsson 1987). When comparing such data with models of clast dispersal, an approximation is introduced since existing models refer to the average of the three main axes of each clast (Wilson and Huang 1979; Wilson and Walker 1987), for which MP and ML are only crude estimates. To evaluate the degree of approximation we repeated measurements of MP and ML at seven points at one locality 10 km south of the caldera rim. This locality was chosen because of the particularly good exposure and because it appears to have been unaffected by ballistic clasts. In each of the seven 0.5 m^2 fallout areas we also measured the length of the three main axes of the five largest clasts; the greatest value of the average of the three axes is referred to as A (AP for pumice, AL for lithics), while M refers to the average of the maximum length of the five largest clasts (MP for pumice, ML for lithics) (Table 1, Fig. 12). The relevant results are:

1. the value of A is always smaller than the corresponding M (in one case they coincide);

Table 1. M and A values obtained on seven different 0.5 m^2 surfaces of the BF, at about 10 km southeast of the caldera rim. Values are in cm (except for σ/μ). σ: standard deviation. μ: mean value

Section	M		A	
	MP	ML	AP	AL
1	7.1	4.5	6.1	3.9
2	7.6	3.9	5.7	3.3
3	8.0	4.7	8.0	4.1
4	7.5	5.0	6.5	4.5
5	8.8	4.5	8.3	4.1
6	7.1	4.0	6.5	3.2
7	9.6	4.2	7.1	3.6
σ	0.9	0.4	1.0	0.5
μ	7.96	4.40	6.89	3.81
σ/μ	0.11	0.09	0.15	0.13

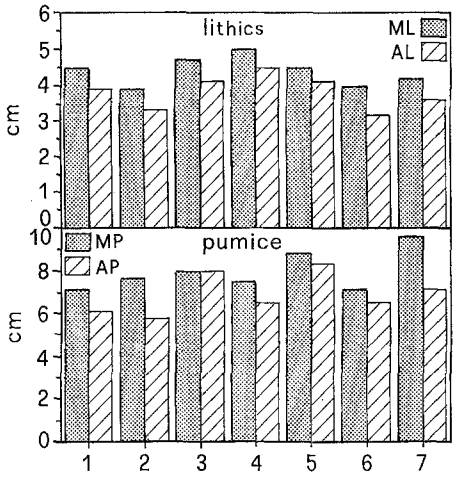

Fig. 12. Bar diagram comparisons between M (average of the five largest diameters) and A (larger value of the average of the three principal axes) for pumice (*P*) and lithics (*L*). Measurements were carried out at a locality about 10 km SE of the caldera rim

2. the standard deviations nearly coincide for M and A;
3. the ratio of standard deviation of M to the mean value of M nearly coincides for pumice and lithics;
4. the highest values of AP and AL among the seven sections closely resemble the average values of MP and ML respectively.

Point 2 suggests that the use of A instead of M does not significantly smooth fluctuations in the measurements. Point 3 indicates that the more regular pattern of pumice isopleths compared to the lithic isopleths of the BF (Fig. 13) is not related to greater variability of the lithic data. Point 4 is the most interesting result: it suggests that the collection of M values is a sufficiently reliable procedure when a large number of stratigraphic sections are available, whereas when they are scarce the collection of A values over a larger (e.g. about 4 m^2) area of the deposit is preferable. Because of the generally good exposure of the BF, we adopted the collection of M values. It is once again evident from the circular pattern of the isopleths (Fig. 13) that the eruption occurred in a near absence of wind.

Pyroclast dispersal models

General characteristics of models

The distribution of pyroclasts close to the vent depends on the characteristics and dynamics of the erupting mixture at the base of the column, whereas the distribution at great distance is a function of both column height and wind velocity (Wilson 1972, 1976; Carey and Sparks 1986; Wilson and Walker 1987). Carey and Sparks (1986) developed a column model (here named 'CS') which makes it possible to distinguish between these last two factors. This model takes into account both the distortion of the clast support envelope by wind and the expansion of the plume at the neutral buoyancy level. Furthermore, clast trajectories are adjusted to take into account the additional radial expansion of the umbrella region due to the lateral forced intrusion of the plume into the atmosphere. Two parameters of each isopleth must be considered: the half maximum width perpendicular to the axis of dispersion ('crosswind range') and the maximum distance from the vent ('downwind range'). The model wind velocity depends on the vertical profile of the wind itself, which

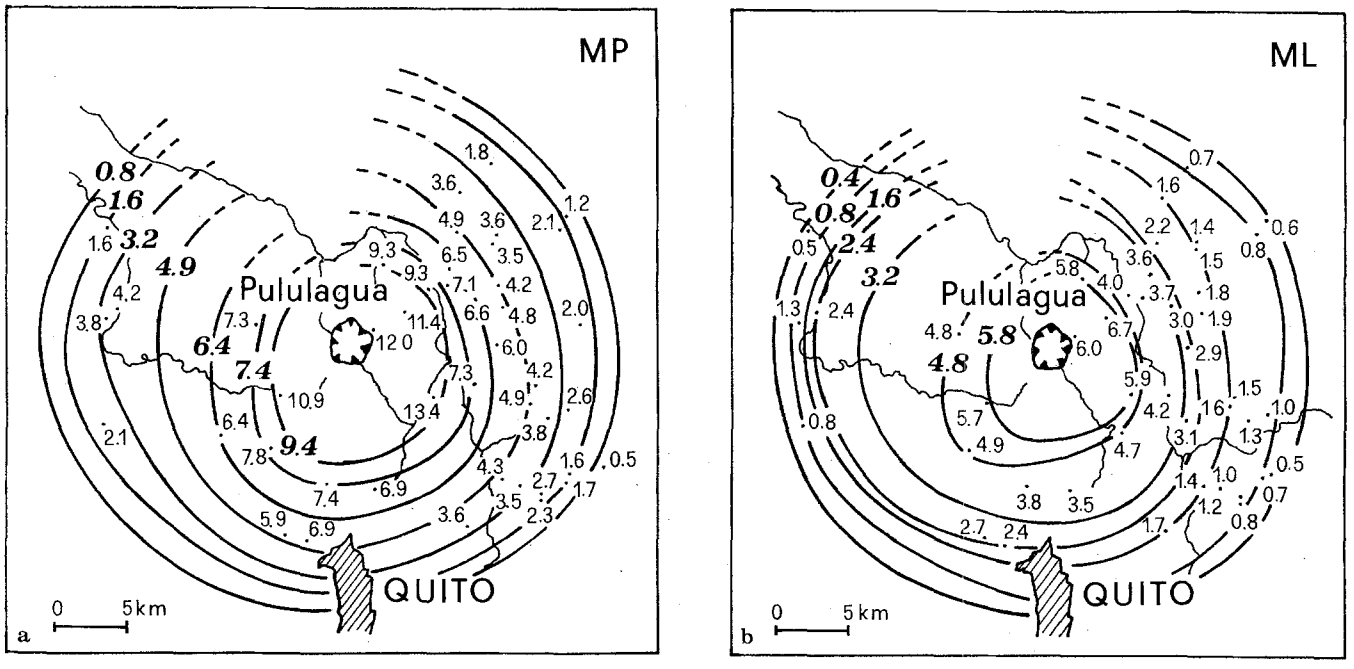

Fig. 13a, b. MP and ML isopleth maps of the BF. Values (in cm) were obtained by averaging the maximum diameter of the five largest clasts collected on a 0.5 m^2 surface

must be arbitrarily assumed or based on current-day atmospheric profiles for unobserved eruptions. In contrast, the model column height depends only on the crosswind range, and is not a function of the assumed wind profile. Since pumice clasts cause some complications due to density variations with size or possible breakage upon impact, the CS model preferentially uses lithic isopleths.

A somewhat simpler and yet more complete use of the clast-size data can be achieved if isopleths are plotted in a 'ln diameter-area$^{1/2}$' ('ln D-A$^{1/2}$') diagram. Indeed, not only the thickness, but also the theoretical grainsize distribution of a fall deposit as obtained by Carey and Sparks (1986), tends to follow a simple exponential decrease law (Pyle 1989). Points on the 'ln D-A$^{1/2}$') diagram therefore approximate to a straight line the slope of which depends on column height and wind velocity during the eruption. In reality, the interpretation of points relative to pumice isopleths is more complex due to the above-mentioned complications.

Wilson and Walker (1987) proposed a model (here named 'WW') which relies on different assumptions about the velocity distribution inside the column, and which does not take into account further radial expansion in the umbrella region. Their theoretical curves apply only to the material released by the lower part of the column, which does not enter the umbrella region. The agreement between the estimates of mass flux obtained by WW and CS is good for all the modeled eruptions; however, WW model yields a column height which is systematically lower by about 15% than that obtained by the CS model. This difference is attributed by Wilson and Walker (1987) to the fact that the CS model correlates the mass flux to the height of the column by assuming a greater value for the fraction of particles retained in the column at a given height, and hence assigning a higher efficiency to the conversion of thermal into mechanical energy.

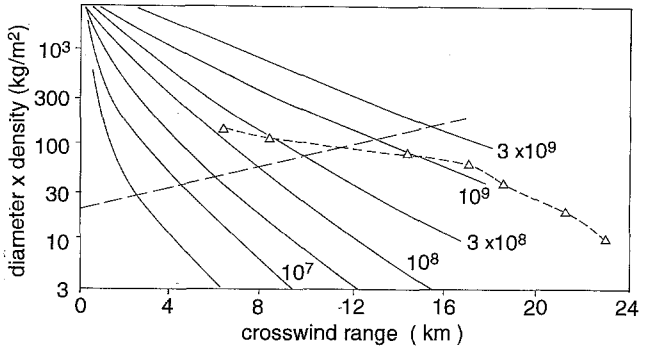

Fig. 14. Crosswind range vs the product 'diameter × density' for ML isopleths of the BF (after Wilson and Walker 1987)

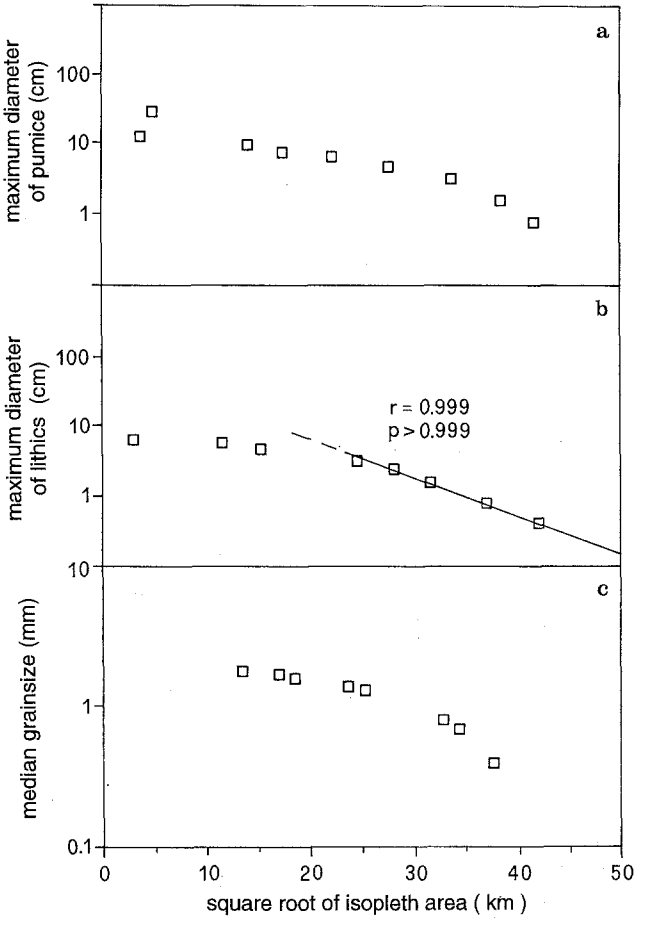

Fig. 15. 'Square root of isopleth area vs **a** lnMP; **b** lnML; **c** lnMedian diameter' diagram for the BF (after Pyle 1989)

Application to the Pululagua basal fallout

From Fig. 14 it is possible to obtain, for each mass flux, the limiting value of the product 'diameter × density' of clasts which, according to WW, enter the umbrella region and hence undergo further radial expansion in accordance with the model of forced intrusion. This limiting value corresponds to the intercept between a given mass discharge rate curve and the diagonal dashed line on Fig. 14. For clasts with a 'diameter × density' value lower than the limiting value, CS trends do apply, and these clasts therefore will follow an exponential decrease law as shown by Pyle (1989). In the range of mass fluxes related to column heights between 30 and 36 km (about 1.4-5 × 10^8 kg s^{-1}) — the probable range for the first plinian eruption of Pululagua — and assuming a constant density of 2500 kg m^{-3} for lithic clasts, the maximum dimension of clasts which reach the level of neutral buoyancy ranges between 2 and 3 cm in diameter. If we now refer to Fig. 15b, we find that only the last four isopleths (2.4-, 1.6-, 0.8- and 0.4-cm) lie on a straight line, in very good agreement with both Wilson and Walker's (1987) and Pyle's (1989) arguments. The shift from this line is small for the 3.2-cm isopleth, but it becomes significant for greater diameters. A similar although less sharp trend is shown by pumice isopleths (Fig. 15a) as well as the isopleths for the median diameter of grains (Fig. 15c). Figure 15c has been obtained by considering circular curves with a radius equal to the isopleth radius in the SW direction, in an attempt to eliminate the above-

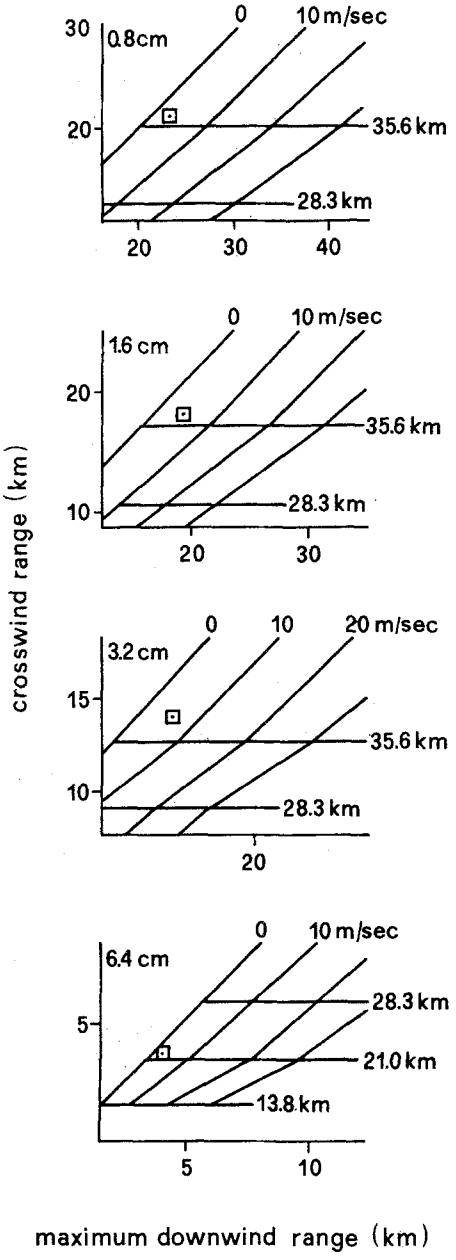

Fig. 16. 'Crosswind range–maximum downwind range' diagram for ML isopleths of the BF (after Carey and Sparks 1986)

mentioned complexities caused by the process of contamination by fines. The most proximal point in Fig. 15a, b represents an isopleth which is constructed on the basis of only one measurement by assuming a general circular pattern. It relates to the northeastern section which was sheltered from ballistic clasts; even in this case, the agreement with the general trend is very good. The slope given by the linear trend in Fig. 15b is equal to 0.13, which corresponds to a 'clast half distance' b_c (as defined by Pyle 1989) equal to 3.01. By fitting an empirical function between points on theoretical dispersal curves from CS, Pyle (1989) defines a relationship between b_c and the height Hb of the level of neutral buoyancy, which gives Hb = 20.5 km. From the relation maximum column height, Ht = Hb/0.7 (Sparks 1986) we then obtain Ht = 29.3 km. In Fig. 16 lithic data are plotted on the 'crosswind range – downwind range' diagram of CS. In accordance with the above discussion, the 6.4-cm isopleth yields a significantly lower column height (about 21 km) as compared to that obtained by the 3.2-, 1.6- and 0.8-cm isopleths, which all give a column height of 36 km. The discrepancy between this height and the one (Ht = 29 km) previously obtained is probably due to a number of causes. In this case Ht has been obtained directly, whereas previously it was obtained from Hb by means of a relationship that contains a margin of approximation. Furthermore, the diagram in Fig. 16 must also be constrained by clast density, whereas Fig. 15 lacks this dependence. In any case the model estimates of column height are probably only correct to within 10–20% due to the great number of variables which play a role in the process (Woods 1988; Carey and Sigurdsson 1989). Thus the most probable value for the maximum CS model column height can be hypothesized to be about 32–33 km.

If we now derive a mass flux from this value by using the efficiency of transformation of thermal into mechanical energy proposed by Sparks (1986), we obtained $M = 2 \times 10^8$ kg s^{-1}. This is obtained from the distal distribution of clasts, which is in good agreement with an exponential decrease law.

The distribution of clasts which did not reach neutral buoyancy height but were released from lower regions of the eruption column, is better described by the WW model. The agreement with CS is very good for estimation of the mass discharge rate, the value of which must be obtained using only points above the dashed line in Fig. 14. WW, however, assume a less efficient transformation of thermal into mechanical energy and from their equation we obtain Ht = 28 km.

The values thus obtained for the maximum column height, Ht = 32–33 km from CS and Ht = 28 km from WW, should be considered as upper and lower limits, respectively. The CS model gives higher column heights since it does not take into account heat lost from clasts in the lower regions of the column, while the WW model gives lower model heights since it implies a greater entrainment of air which tends to attenuate the upward momentum (Wilson and Walker 1987).

Discussion

Comparison between models of tephra dispersal from eruptive columns (Sparks 1986; Carey and Sparks 1986; Wilson and Walker 1987; Pyle 1989) and data from the BF of Pululagua shows that a simple exponential law seems suitable to describe the thickness of the deposit, whereas for clast dispersal an exponential decrease only occurs below a critical particle diameter. This fits with Wilson and Walker's (1987) model and implies some restrictions in the use of the 'ln D-$A^{1/2}$' plots to obtain maximum column height. Indeed, we

emphasize the necessity of obtaining the exact slope on such a diagram, implying that the geometry of isopleths must be well established in proximal and distal zones. The use of only a few or just two isopleths is not sufficient as seemed initially justified by Pyle's (1989) work. The same can be said about the use of crosswind and maximum downwind range diagrams proposed by Carey and Sparks (1986).

It is not clear why some eruptions seem to show a linear trend from proximal to distal zones. It is possible that the presence of wind tends to modify the true distribution of clasts, by acting with greater efficiency on smaller clasts as a consequence of both their lower inertia and longer time spent in the atmosphere. In such a case the value of the horizontal axis in a 'lnD-$A^{1/2}$' plot would increase progressively for distal points, and hence points tend to approximate to a straight line, the slope of which is less than that of a curve for the same column height under no-wind conditions. This would produce an overestimation of column height. This idea is supported by the clast distribution pattern of the Taupo ultraplinian deposit. Here clasts less than 5 cm in diameter were transported to more than 150 km from the vent (Walker 1980), while subjected to a wind with an estimated velocity of almost 30 m s^{-1} (Carey and Sparks 1986). On a 'lnD-$A^{1/2}$' diagram the 4-cm isopleth (the most well constrained distal one) is strongly displaced from the linear trend in favour of a larger dispersion (Fig. 17). The Fogo A deposit is also of particular interest since it represents another case of no-wind conditions during a plinian eruption, and was used by Carey and Sparks (1986) to test their model. Unfortunately the island of São Miguel (Azores) on which Fogo A is located has an elongate form which provides only a partial picture of the distribution pattern. The well-constrained lithic isopleths are only those greater than 10 cm, and we can arrive only by extrapolation at the 5-cm isopleth (Walker and Croasdale 1971). The use of a diagram like Fig. 14 is more suitable to furnish correct information on column energetics in such cases.

The good aggrement between the CS and WW models for the determination of mass flux is confirmed, and Fig. 15b suggests that a significant proportion of coarse clasts are released before reaching the top of the column. This implies that the conversion of thermal into mechanical energy is better described by WW than by the equation proposed by Sparks (1986).

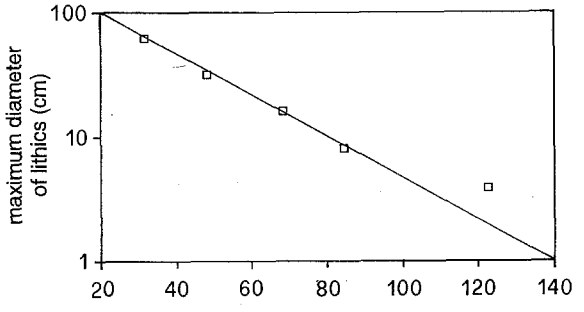

Fig. 17. 'lnML vs square root of isopleth area' diagram for Taupo fall layer; data from Walker 1980

Summary and conclusions

This work focused on the plinian Basal Fall (BF) of Pululagua. Its dispersal indicates a near absence of wind during eruption; this leads to the possibility of obtaining especially reliable data not complicated by the effect of wind. The fall deposit is characterized everywhere by a finer top passing gradationally into a fine ash layer, which is interpreted to comprise the finest portion of the material originally contained in the column; this was favoured by the unusual no-wind conditions existing during the eruption. Grainsize characteristics and the dispersal pattern of the basal fall of Pululagua were investigated, and the results were applied to models of clast dispersal. The major results are:

1. the characteristics of the deposit concur to suggest nearly no-wind conditions during its emplacement;
2. grainsize characteristics of the lapilli fall layer do not differ significantly from other plinian deposits. The only departure is shown by the trend of the median diameter of clasts, and is explained by contamination by ash in the region northeast of the vent, possibly due to partial collapses of the eruptive column which formed surges;
3. a simple exponential decrease of thickness with distance as proposed by Pyle (1989) for plinian falls fits well with the BF;
4. the same law is followed by maximum lithic clasts but only below a critical size of about 3 cm, suggesting that only a small proportion of large clasts were able to reach the top of the column;
5. point 4 implies that, in order to obtain column heights by clast dispersal models, the clast distribution must be well established in proximal and distal zones. Knowledge of only a few or just two isopleths, regardless of their distance from vent, is not sufficient.

Acknowledgements. The authors are grateful to INEMIN (Instituto Nacional Ecuadoriano de Mineria) for having provided logistical support and assistance during the fieldwork. Steven Carey, David Pyle and Judy Fierstein provided many helpful comments on a previous version of the paper. We also thank G La Volpe for having kindly provided fine-grained granulometric data with a Coulter Counter TA II instrument.

References

Barberi F, Cioni R, Rosi M, Santacroce R, Sbrana A, Vecci R (1989) Magmatic and phreatomagmatic phases in explosive eruptions of Vesuvius as deduced by grain-size and component analysis of the pyroclastic deposit. J Volcanol Geotherm Res 38:287–307

Barberi F, Coltelli M, Ferrara G, Innocenti F, Navarro JM, Santacroce R (1988) Plio-Quaternary volcanism in Ecuador. Geol Mag 125:1–14

Carey S, Sigurdsson H (1980) The Roseau Ash: deep-sea tephra deposits from a major eruption on Dominica, Lesser Antilles arc. J Volcanol Geotherm Res 7:67–86
Carey S, Sigurdsson H (1987) Temporal variations of column height and magma discharge rate during the 79 AD eruption of Vesuvius. Geol Soc Am Bull 99:303–314
Carey S, Sigurdsson H (1989) The intensity of plinian eruptions. Bull Volcanol 51:28–40
Carey S, Sparks RSJ (1986) Quantitative models of the fallout and dispersal of tephra from volcanic eruption columns. Bull Volcanol 48:109–125
Carey S, Sigurdsson H, Sparks RSJ (1988) Experimental studies of particle laden plumes. J Geophys Res 93, B12:15314–15328
Crandell DR, Mullineaux DR (1973) Pine Creek volcanic assemblage at Mount St. Helens, Washington. US Geol Surv Bull 1383-A:1–23
Fisher RV, Glicken HX, Hoblitt RP (1987) May 18, 1980, Mount St Helens deposits in South Coldwater Creek, Washington. J Geophys Res 92, B10:10267–10283
Froggatt PC (1982) Review of methods of estimating rhyolitic tephra volumes; applications to the Taupo Volcanic Zone, New Zealand. J Volcanol Geotherm Res 14:301–318
Geotermica Italiana-INEMIN (1989) Mitigacion del Riesgo Volcanico en el Area Metropolitana de Quito. Ministero degli Affari Esteri-DGCS. Pisa
Hall ML (1977) El volcanismo en el Ecuador. IPGM Seccion Nacional del Ecuador, Quito
Houghton BF, Wilson CJN (1989) A vesicularity index for pyroclastic deposits. Bull Volcanol 51:451–462
Howorth R (1975) New formations of Late Pleistocene tephras from the Okataina Volcanic Centre, New Zealand. N Z J Geol Geophys 18 (5):683–712
Isaacson JS (1987) Volcanic activity and human occupation of the Northern Andes: the application of tephrostratigraphic techniques to the problem of human settlement in the Western Montaña during the Ecuadorian Formative. PhD thesis, University of Illinois
Morton BR, Taylor G, Turner JS (1956) Turbulent gravitational convection from maintained and instantaneous sources. Phil Trans R Soc London Ser A 234:1–23
Pyle DM (1989) The thickness, volume and grainsize of tephra fall deposits. Bull Volcanol 51:1–15
Rose WI, Bonis S, Stoiber RE, Keller M, Bickford T (1973) Studies of volcanic ash from two recent Central America eruptions. Bull Volcanol 37:338–364
Rosi M (1992) A model for the formation of vesiculated tuff by coalescence of accretionary lapilli. Bull Volcanol 54:429–434
Self S, Sparks RSJ (1978) Characteristics of widespread pyroclastic deposits formed by the interaction of silicic magma and water. Bull Volcanol 41:196–212
Settle M (1978) Volcanic eruption clouds and the thermal output of explosive eruptions. J Volcanol Geotherm Res 3:309–324
Simkin T, Siebert L, McClell L, Bridge D, Newhall C, Latter JH (1981) Volcanoes of the world. Stroudsburg, Pennsylvania: Hutchinson Ross 232 pp
Sparks RSJ (1986) The dimensions and dynamics of volcanic eruption columns. Bull Volcanol 48:3–15
Suzuki T, Katsui Y, Nakamura T (1973) Size distribution of the Tarumai Ta-b pumice-fall deposit. Bull Volcanol Soc Japan 18:47–64
Villalba M (1988) Cotocollao: una aldea formativa del valle de Quito. Museo del Banco Central del Ecuador, Quito
Vucetich CG, Pullar WA (1973) Holocene tephra formations erupted in the Taupo area, and interbedded tephras from other volcanic sources. N Z J Geol Geophys 16:745–780
Walker GPL (1971) Grainsize characteristics of pyroclastic deposits. J Geol 79:696–714
Walker GPL (1980) The Taupo pumice: product of the most powerful known (ultraplinian) eruption? J Volcanol Geotherm Res 8:69–94
Walker GPL (1981) Plinian eruptions and their products. Bull Volcanol 44-2:223–240
Walker GPL (1983) Ignimbrite types and ignimbrite problems. J Volcanol Geotherm Res 17:65–88
Walker GPL, Croasdale R (1971) Two Plinian-type eruptions in the Azores. J Geol Soc London 127:17–56
Williams H (1960) Volcanic history of the Guatemalan Highlands. Univ Calif Publ Geol Sci 38:1–87
Wilson L (1972) Explosive volcanic eruptions — II. The atmospheric trajectories of pyroclasts. Geophys J R astr Soc 30:381–392
Wilson L (1976) Explosive volcanic eruptions — III. Plinian eruption columns. Geophys J R astr Soc 45:543–556
Wilson L (1980) Relationships between pressure, volatile content and ejecta velocity in three types of volcanic explosions. J Volcanol Geotherm Res 8:297–313
Wilson L, Huang TC (1979) The influence of shape on the atmospheric settling velocity of volcanic ash particles. Earth Planet Sci Lett 44:311–324
Wilson L, Walker GPL (1987) Explosive volcanic eruptions — VI. Ejecta dispersal in plinian eruptions: the control of eruption conditions and atmospheric properties. Geophys J R astr Soc 89:657–679
Wilson L, Sparks RSJ, Huang TC, Watkins ND (1978) The control of volcanic column height by eruption energetics and dynamics. J Geophys Res 83:1829–1835
Woods AW (1988) The fluid dynamics and thermodynamics of eruption columns. Bull Volcanol 50:169–193

Editorial responsibility: B. F. Houghton